Theory of electron energy spectrum of IV–VI semiconductors

B. A. Volkov, O. A. Pankratov, and A. V. Sazonov

P. N. Lebedev Physics Institute, USSR Academy of Sciences

(Submitted 17 March 1983)
Zh. Eksp. Teor. Fiz. **85**, 1395–1408 (October 1983)

The approach used by Abrikosov and Fal'kovskiĭ [Sov. Phys. JETP **16**, 769 (1963)] is supplemented by premises [Sov. Phys. JETP **48**, 687 (1968)] concerning the genesis of bands of atomic p-states and is used to calculate the electron spectrum of IV–VI semiconductors in multicomponent solid solutions on their basis. The tight-binding approximation is used to establish a correspondence between the parameters of the band structure and the atomic characteristics, and the number of independent parameters of the theory is reduced to a minimum.

PACS numbers: ; 71.25.Tn, 71.25.Cx

1. INTRODUCTION

Investigations of IV–VI semiconductors have been going on for many years. Their band structure, at least in the case of lead salts PB(S, Se, Te) is regarded as established.[1] At the same time, the information accumulated on the structure of energy bands could not be used to explain the structure instabilities, the generation of free carriers by intrinsic defects, and other fundamental properties of the compounds. What was needed was a sufficiently simple explanation of the origin of the energy spectrum, connecting the band and the atomic parameters. Such a model, based on the tight-binding approximation in a basis of atomic p orbitals, was proposed by us in Ref. 2. This model made it possible to understand the nature of the structural phase transitions in (Sn, Ge)Te (Ref. 2), the energy spectrum and the doping caction of vacancies,[3] as well as the anomalies of the dielectric constant[4] in IV–VI compounds. It was found that the approach of Ref. 2 describes the band structure not only qualitatively but also quantitatively, as was demonstrated[5] by numerical interpolation of the PbTe spectrum.

Besides IV–VI compounds, the model of Ref. 2 is applicable to semimetals (Bi, Sb, As) and chalcogenide semiconductors (Te, Se). The similarity of the electron spectra of all these substances is due to the dominant role of the atomic p states in the formation of the valence bonds. Numerical calculations[1)] have shown that near the Fermi filling boundary the energy bands are grouped into triplets that do not overlap with other bands. This means that the splitting of the atomic p levels by the crystal field is less than the distance to bands of other symmetry and the bands closest to the Fermi boundary are made up mainly of p-states.

The bismuth and tellurium crystal lattices are obtained by slight distortions of a simple cubic (sc) structure. This circumstance was used by Abrikosov and Fal'kovskiĭ[9] to develop a deformation theory of the bismuth energy spectrum. According to them, the spectrum of a semimetal is the result of partial dielectrization of the metallic "parent phase" with sc structure as a consequence of the doubling of the period and of the acoustic deformation of the lattice.

The IV–VI semiconductor group includes compounds with cubic NaCl-type structure (lead chalcogenides, SnTe and GeTe in the paraelectric phase), as well as with rhombohedral and orthorhombic structures.[2)] We confine ourselves below to cubic IV–VI compounds. Their electron spectrum can likewise be easily constructed by starting with a parent phase having a sc lattice[2] into which the rock-salt lattice is transformed if the neighboring atoms are regarded as equivalent. The difference between the IV and VI atoms is characterized by the ionicity potential $\Delta(\mathbf{r})$ (Refs. 2, 10), which has the fcc lattice symmetry.[3)] Ionicity plays in IV–VI compounds the same role as the potential $\Delta_{ph}(\mathbf{r})$ due to the shift of the sublattices in bismuth.

In this paper we have applied to IV–VI semiconductors the method of Abrikosov and Fal'kovskiĭ,[9] supplemented by premises concerning the genesis of bands from the p orbitals of the IV and VI atoms. This has enabled us to determine the symmetry of the parent-phase terms at points L of the Brillouin zone (the extremum points of the bands in IV–VI) and avoid the difficulties raised by the Luttinger theorem in the theory for bismuth.[12]

Within the framework of such a model, the dispersion of the six bands near the L point (two p triplets, one above and the other below the Fermi level) is characterized by four matrix elements of the momentum operator. Yet Dimmock's six-band $\mathbf{k}\cdot\mathbf{p}$ scheme[13] based on the binary group D_{3d} contains thirteen independent momentum matrix elements, and the model of Mitchell and Wallis,[14] which starts from the representations of the simple group, has five elements.

The theory becomes further simplified if the tight-binding model is used. In this case only two independent momentum matrix elements appear in the first coordination group, and the remaining two are connected with more remote coordination spheres, starting with the third, and can be neglected because of the rapid decrease of the overlap integrals.

Just as in the Dimmock $\mathbf{k}\cdot\mathbf{p}$ scheme,[13] in our model there are five other independent parameters that determine the energy gap at the L point. The tight-binding approximation, however, permits three of them (the spin-orbit constants $\lambda_{\pm}$ and the ionicity matrix element Δ) to be connected with the atomic characteristics.

Thus, whereas in Dimmock's model the spectrum at the L point is characterized by $13 + 5 = 18$ independent numbers (or by 11, as in Ref. 14), in our scheme only four parameters remain to be determined from experiment. It turns out that two of them, ξ_0 and ξ_1 (see Table I below) are practically the same for all IV–VI compounds.

 0038-5646/83/100809-08$04.00

TABLE I. Values of the model parameters (in eV) for IV–VI compounds. The positions of the L levels corresponding to the listed parameters are given.

	λ_-	λ_+	W_-	W_+	Δ	ξ_0	ξ_1	$L^{4s'}$	$L^{6'}$	$L^{6'}$
PbS	0.424	0.032	−0.46	0.86	1.6	3.76	−0.9	2.49	1.93	0.39
PbSe	0.424	0.140	−0.315	0.65	1.25	3.65	−0.9	1.99	1.54	0.23
PbTe	0.424	0.28	−0.09	0.29	0.876	3.41	−0.9	1.39	1.22	0.014
SnTe	0.158	0.28	−0.075	0.38	0.47	3.5	−0.9	0.7	0.58	0.13

	L^6	L^{45}	L^6	$\frac{\partial \varepsilon_g}{\partial p}\cdot 10^{-6}\frac{\text{eV}}{\text{bar}}$		$m_{p\perp}$	
				theor	exp [1]	theor	exp [1]
PbS	0.11	−2.44	−2.5	−8.7	−8	0.069	0.075±0.01
PbSe	0.065	−1.76	−2.06	−9.2	−8	0.034	0.034±0.007
PbTe	−0.17	−0.89	−1.57	−8.1	−8	0.022	0.028±0.002
SnTe	0.39	−0.57	−1.24	8.7	–	0.13	–

	$m_{p\parallel}$		$m_{n\perp}$		$m_{n\parallel}$		$\lvert\delta\rvert$
	theor	exp [1]	theor	exp [1]	theor	exp [1]	
PbS	0.103	0.11±0.02	0.087	0.08±0.01	0.106	0.105±0.015	1.09
PbSe	0.083	0.068±0.015	0.037	0.04±0.008	0.088	0.07±0.015	0.88
PbTe	0.32	0.24±0.08	0.021	0.028±0.002	0.28	0.24±0.08	0.41
SnTe	0.58	–	–	–	–	–	0.59

Since all the parameters have the meaning of intracenter and intercenter overlap integrals, they can be interpolated as functions of the chemical composition or of the lattice periods. This enabled us to calculate the energy spectra of multicomponent solid solutions. In this paper we present the results for ternary alloys. We obtain also the form of the energy spectrum of PbPo.

2. DIELECTRIZATION OF THE SPECTRUM. ENERGY LEVELS AT THE L POINT

Just as bismuth, IV–VI compounds have on the average three valence p electrons per atom. Therefore the initial sc corresponds to the same metallic parent phase. To determine the form of the bare spectrum in the entire Brillouin zone we use the tight-binding approximation in a basis of localized p functions. The information on the symmetry of the initial terms at the singular points is then obviously not connected with this approximation and remains exact.

The three p bands $\xi_n(\mathbf{k})$ (the band indices $n = x, y, z$ correspond to the cubic coordinate axes) are made up of localized functions $f_n(\mathbf{r}-\mathbf{R})$ that are centered in sites $\mathbf{R}$ of the sc lattice and transform in accord with the vector representation of the cube group. If the index n were to remain a "good" quantum number in the crystal, the Fermi surface would consist of three pairs of corrugated planes perpendicular to the cubic axes[2,5] (Fig. 1). The band extrema in IV–VI semiconductors are located precisely at the intersection points of these planes (the L points), at which the degeneracy of the initial spectrum is a maximum. Eight L points have coordinates $\mathbf{q}_i/2$, where the vectors $\mathbf{q}_i$ are obtained by the cube-group operations from the vector $\mathbf{q} = (\pi/a)\,(111)$, where a is the period of the sc lattice.

The functions

$$\varphi_{n\mathbf{k}}(\mathbf{r}) = \frac{1}{\sqrt{N}}\sum_{\mathbf{R}} e^{i\mathbf{k}\mathbf{R}} f_n(\mathbf{r}-\mathbf{R}), \tag{1}$$

taken at $\mathbf{k} = \mathbf{q}/2$ (N is the number of sites of the sc lattice) generate a three-dimensional representation Γ of the small group C_{3v} of the L point. The mixing of the states (1) with different n (hybridization of the bands) lifts the accidental degeneracy[4]:

$$\Gamma = A_1 + E. \tag{2}$$

The bare Fermi surface (Fig. 1) splits then into two closed surfaces and one open one. At the L point one of the closed surfaces is tangent to the open one (Fig. 2).

Inclusion of the ionicity (or of Δ_{ph} in the case of bismuth) changes the translational periodicity of the crystal. The volume of the Brillouin zone is decreased by one-half. For the model spectrum[2,5] (the lattice constant in the expression $\mathbf{k}a$ will be omitted here and elsewhere):

$$\xi_x(\mathbf{k}) = \xi_0 \cos k_x + \xi_1(\cos k_y + \cos k_z) \tag{3}$$

($\xi_{y,z}$ are obtained by cyclic permutation of the subscripts); it is easy to verify that the arithmetic mean of the volumes of the closed Fermi surfaces 1 and 2 (Fig. 2) is equal to the volume of the new Brillouin zone, just as the volume of the

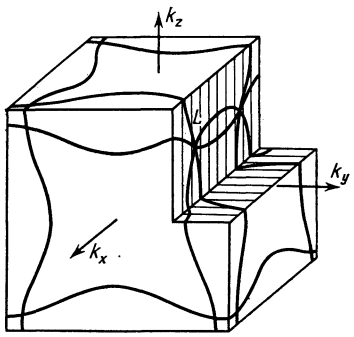

FIG. 1. Bare Fermi surface of cubic parent phase.

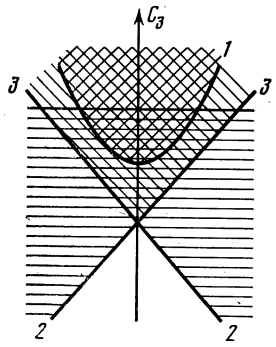

FIG. 2. Scheme of Fermi surface of the parent phase in the vicinity of the L point.

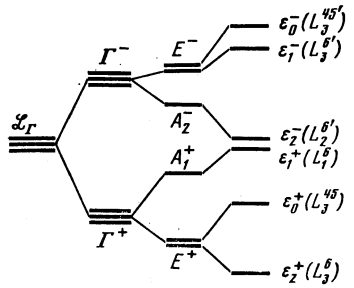

FIG. 3. Genesis of electron spectrum at the L point following successive turning-on of ionicity, hybridization, and spin-orbit interaction.

filled states for the open Fermi surface 3. Therefore the dielectrization of the spectrum is due to the superposition of the closed surfaces on each other upon translation by the vector $\mathbf{q}$. The open surface is self-congruent in this case.

Abrikosov and Fal'kovskiĭ[9] started with one representation of E, assuming congruence of the Fermi surfaces that are dexenerate at the L point. This assumption, however, led to a contradiction with the rule for the filling of the Brillouin zones when the spectrum is dielectrized (the Luttinger theorem). To get around this difficulty, Abrikosov[12] introduced one more Fermi surface (level A_1 at the L point), which became dielectrized by itself with doubling of the period. The position of the level A_1 was chosen such that it did not influence the form of the spectrum at the band edges.

In fact, as can be seen from Figs. 1 and 2, the doublet term E is produced by the intersection of an open Fermi surface with the closed one that cannot vanish when the period is doubled. The third surface corresponding to the level A can likewise not become dielectrized by itself, but turns out to be congruent with the closed surface that is degenerate at the L point. Thus, an essential role in the formation of the dielectric spectrum is played by all three Fermi surfaces and, according to (2), the basis set of functions should contain the terms A_1 and E.

In an NaCl-type structure, L points separated by a vector $\mathbf{q}$ are equivalent. Accordingly there appears to the small group an inversion operation that transforms it into the group D_{3d}. This group has six irreducible representations $A_1^{\pm}, A_2^{\pm}, E^{\pm}$ (the superscript labels respectively the even and odd representations). In the parent phase the eigenfunctions $\Psi_{q/2}^{(i)}$ at the L point are transformed in accord with the irreducible representations of the group C_{3v}. Combining the functions $\Psi_{\pm q/2}$ belonging to equivalent points, we obtain reducible representations of a new small group D_{3d}, which break up into irreducible ones:

$$\mathscr{L}_{A_1}=A_1^+ + A_2^- \to L_1^6 + L_2^{6'}, \tag{4}$$

$$\mathscr{L}_E=E^+ + E^- \to L_3^{45} + L_3^6 + L_3^{6'} + L_3^{45'}. \tag{5}$$

The arrows indicate transitions to representations of a binary group in the notation adopted for the L point.[1] The doublet terms $E^{\pm}$ are split by the spin-orbit (SO) interaction and a set of six levels is produced.

It will be shown below that in IV–VI semiconductors the splitting due to the ionicity exceeds the hybridization and the SO interactions.[5)] It is therefore convenient to change the sequence of turning on the interactions and start with the ionicity, which splits the reducible representation $\mathscr{L}_\Gamma$ made up by triplets of equivalent L points into even and odd parts:

$$\mathscr{L}_\Gamma=\Gamma^+ + \Gamma^-. \tag{6}$$

The hybridization $\hat{W}$ splits next the triplets

$$\Gamma^+=A_1^+ + E^+, \tag{7}$$

$$\Gamma^-=A_2^- + E^- \tag{8}$$

and the SO interaction $\hat{\lambda}$ lifts the degeneracy of the $E^{\pm}$ levels in analogy with (5) (Fig. 3).

Taking (6) into account, it is convenient to change from the basis (1) to the functions

$$\varphi_{\mathbf{n},\mathbf{k}}^{\pm}=(\varphi_{n,\mathbf{k}+\mathbf{q}/2} \mp \varphi_{n,\mathbf{k}-\mathbf{q}/2})/\sqrt{2}, \tag{9}$$

which have a definite parity at the L point (this is now the point $\mathbf{k}=0$, since (9) includes a shift of the origin in $\mathbf{k}$-space). We denote the functions that are even and odd at $\mathbf{k}=0$ by φ_n^+ and φ_n^- (when symmetrizing in (9) it must be borne in mind that the p orbitals $f_n(\mathbf{r})$ are odd).

We construct an equivalent Hamiltonian $\hat{\mathscr{H}}_{\pm}$ (for even and odd states) whose matrix elements in the basis $\varphi_n^{\pm}\uparrow,\downarrow$ coincide with the matrix elements of the crystal Hamiltonian $\hat{H}+\hat{\lambda}$ ($\uparrow$ and $\downarrow$ are spin functions).

By virtue of the symmetry, all the off-diagonal elements $H_{nn'}$ are equal to one another. Therefore the hybridization operator $\hat{W}$ can be expressed in terms of the operator $\hat{C}_3$ of rotation about a threefold axis:

$$\hat{W}_{\pm}=W_{\pm}(\hat{C}_3+\hat{C}_3^{-1})=2W_{\pm}\cos(^2/_3\pi\mathbf{Ln}),$$

where L is the angular-momentum operator and $n=(1,1,1)\sqrt{3}$. The operator of the SO interaction

$$\hat{\lambda}=-i(\hbar/2mc)^2([\nabla V(\mathbf{r}),\nabla]\boldsymbol{\sigma}), \tag{10}$$

(where $\boldsymbol{\sigma}=(\sigma_x,\sigma_y,\sigma_z)$, σ_n are Pauli matrices, and $V(\mathbf{r})$ is the crystal potential) is equivalent in the $\varphi_n^{\pm}\uparrow,\downarrow$ basis to $\lambda_{\pm}(\mathbf{L}\cdot\boldsymbol{\sigma})$. As a result we obtain

$$\hat{\mathscr{H}}_{\pm}=2W_{\pm}\cos(^2/_3\pi\mathbf{Ln})+\lambda_{\pm}(\mathbf{L}\boldsymbol{\sigma})\mp\Delta. \tag{11}$$

This expression coincides with the Hamiltonian that describes the anomalous Zeeman effect, except that the interaction with the "magnetic field" $(\mathbf{L}\cdot\mathbf{n})$ is under the cosine sign (this preserves the Kramers degeneracy). Using the

known equations for the p-level splitting in a magnetic field, we obtain the spectrum

$$\varepsilon_0^+ = -\Delta + \lambda_+ - W_+,$$

$$\varepsilon_{1,2}^+ = -\Delta + {}^1/_2\{W_+ - \lambda_+ \pm [9W_+^2 + 6W_+\lambda_+ + 9\lambda_+^2]^{1/2}\}, \quad (12)$$

for odd states all the quantities have a minus subscript and we must make the substitution.

In the six-band **k·p** scheme, which is constructed in the basis of the symmetry functions $\{A_1^+, E^+\}$ and $\{A_2^-, E^-\}$, there are two different SO parameters $\Delta_{1,2}^{\pm}$ (Ref. 14). In our model they coincide and are equal to $\lambda_\pm$, because the terms stem from the Γ triplet. The point is that the basis functions constructed in accord with (6)–(8) are not basis functions of general form for the irreducible representations of the group D_{3d}. For matrix elements between functions of like parity this leads to the equality $\Delta_1^{\pm} = \Delta_2^{\pm} = \lambda_\pm$. Of importance for interband matrix element of the momentum operator is the connection between φ_n^+ and φ_n^-:

$$\varphi_n^{\pm}(\mathbf{r}+\boldsymbol{\tau}) = e^{i\mathbf{q}\boldsymbol{\tau}/2}\varphi_n^{\mp}(\mathbf{r}), \quad (13)$$

where $\boldsymbol{\tau} = a(111)$. Because of this relation, four independent elements remain in place of five.[14] It must be emphasized that these restrictions are dictated only by symmetry, and forgoing them within the framework of the six-band model is an exaggeration of the accuracy. More stringent requirements on the basis functions and correspondingly a more substantial decrease of the number of parameters occur when relations (4) and (5) between the representations of the initial and resultant small groups are not in one-to-one correspondence. This situation obtains when the period of the parent phase is tripled in tellurium.

3. ELECTRON SPECTRUM AT BAND EDGES. EFFECTIVE MASSES

The energy spectrum of a crystal consists as a rule of a group of bands that can be characterized by a definite symmetry. The symmetry of the band as a whole is determined by the symmetry of the local functions in the sum (1). The aggregate of the orbitals $|n, \mathbf{R}\equiv f_n(\mathbf{r}-\mathbf{R})$ realizes an infinite-dimensional representation of a space group. Such representations, which are irreducible in the basis of local orbitals, are known as "band" representations.[15] In IV–VI semiconductors six bands closest to the Fermi boundary correspond to a band representation generated by a vector representation of the cube group. Accordingly, the basis functions of this representations serve as a convenient set for determining the spectrum.

If the functions $f_n(\mathbf{r})$ are taken to mean atomic orbitals, the representation (1) is equivalent to the tight-binding approximation. It is more consistent, however, to render concrete only the symmetry $f_n(\mathbf{r})$ and use a definition wherein the basis $|n,\mathbf{R}>$ is orthonormalized.[16] We define the parent-phase Hamiltonian $\hat{h}(\mathbf{r})$ and the ionicity potential $\Delta(\mathbf{r})$ by the relations

$$\hat{h}(\mathbf{r}) = {}^1/_2[H(\mathbf{r}) + H(\mathbf{r}+\boldsymbol{\tau})] = \hat{\mathbf{p}}^2/2m + \mathcal{V}^0(\mathbf{r}), \quad (14)$$

$$\Delta(\mathbf{r}) = {}^1/_2[H(\mathbf{r}) - H(\mathbf{r}+\boldsymbol{\tau})]. \quad (15)$$

The overlap integrals

$$h_{nn'}(\mathbf{R}) = \langle n, \mathbf{R}|h|n', 0\rangle,\ \Delta_{nn'}(\mathbf{R}) = \langle n, \mathbf{R}|\Delta|n', 0\rangle$$

must be regarded as parameters determined by interpolation of the spectrum over the experimental data. Such a procedure[5] shows that they decrease rapidly with increasing $|\mathbf{R}|$, so that two coordinate spheres (CS) suffice.

In the representation (9), the Hamiltonian $\hat{H} + \hat{\lambda}$ takes the form

$$\sum_{\mathbf{R}} e^{i\mathbf{k}\mathbf{R}} \begin{pmatrix} \cos\frac{\mathbf{qR}}{2} - i\sin\frac{\mathbf{qR}}{2} & \\ -i\sin\frac{\mathbf{qR}}{2} - \cos\frac{\mathbf{qR}}{2} & \end{pmatrix} \begin{pmatrix} h_-(\mathbf{R}) & 0 \\ 0 & h_+(\mathbf{R}) \end{pmatrix} \otimes \hat{1} + \begin{pmatrix} \hat{\lambda}_- & 0 \\ 0 & \lambda_+ \end{pmatrix}, \quad (16)$$

where $\hat{1}$ is a unit matrix in spin space and

$$h_\mp(\mathbf{R}) = h_{nn'}(\mathbf{R}) \pm \Delta(\mathbf{R}), \quad (17)$$

$$\hat{\lambda}_\pm = -i\lambda_\pm \begin{pmatrix} 0 & \sigma_z & -\sigma_y \\ -\sigma_z & 0 & \sigma_x \\ \sigma_y & -\sigma_x & 0 \end{pmatrix}. \quad (18)$$

The sequence of the basis function in (16) and (18) is: $\varphi_x^-\uparrow$, $\varphi_x^-\downarrow$, $\varphi_y^-\uparrow$,..., $\varphi_x^+\uparrow$, $\varphi_x^+\downarrow$ $\varphi_y^+\uparrow$,..., where the spinors are defined relative to the cubic axis z.

The exponential in (16) can be expanded in the vicinity of the L point in a series. The diagonal blocks take the form

$$H_\pm = \hat{1}\otimes\sum_{\mathbf{R}}\left[1 - \frac{(\mathbf{kR})^2}{2}\right]\cos\frac{\mathbf{qR}}{2}\,h_\pm(\mathbf{R}) + \hat{\lambda}_\pm, \quad (19)$$

and the off-diagonal the form

$$\xi_\pm = -\hat{1}\otimes\sum_{\mathbf{R}}(\mathbf{kR})\sin(\mathbf{qR}/2)\,h_\pm(\mathbf{R}). \quad (20)$$

The sum contains contributions of the zeroth ($\mathbf{R}_0 = 0$), second [$\mathbf{R}_2 = a(110)$], and succeeding even CS. Contributing to (20) are the first [$\mathbf{R}_1 = a(100)$], third [$\mathbf{R}_3 = a(100)$], and succeeding odd CS. This due to the structure of the functions:

$$\varphi_n^{\pm}(\mathbf{r}) = \sqrt{\frac{2}{N}}\sum_{\mathbf{R}}\begin{Bmatrix} i\sin(\mathbf{qR}/2) \\ \cos(\mathbf{qR}/2) \end{Bmatrix} f_n(\mathbf{r}-\mathbf{R}). \quad (21)$$

Since $\sin(\mathbf{q}\cdot\mathbf{R}/2)\neq 0$, the basis function φ_n^+ is made up only of IV orbitals and φ_n^- of IV orbitals only when $\mathbf{R}$ runs through the VI sublattice and $\cos(\mathbf{q}\cdot\mathbf{R}/2)\neq 0$ on the IV sublattice (the origin is centered in the IV metal). Confining ourselves in (19) and (20) to two CS ($\mathbf{R}_{0,1,2}$), we obtain

$$(\hat{H}_\pm(\mathbf{k}))_{nn'} = \hat{1}\otimes W_\pm\left(1 - \frac{k_n^2 + k_{n'}^2}{2}\right)(1-\delta_{nn'}) + (\eta_n^{\pm}(\mathbf{k}) \pm \Delta)\,\delta_{nn'} + \lambda_\pm, \quad (22)$$

$$\eta_x^{\pm}(\mathbf{k}) = \eta_1^{\pm}(k_y + k_z)k_x + \eta_2 k_y k_z.$$

In this approximation the off-diagonal blocks in (16) are

$$(\xi_\pm)_{nn'} \equiv \hat{\xi}_{nn'} = \xi_n\delta_{nn'}\otimes\hat{1},$$

$$\xi_x = \xi_0 k_x + \xi_1(k_y + k_z). \quad (23)$$

The quantities $\eta_{y,z}$ and $\xi_{y,z}$ are obtained from η_x and ξ_x by cyclic permutation of the indices. All the introduced parameters are expressed in terms of the intra- and intercenter integrals:

$$\Delta=\langle x,\ 0|\Delta(\mathbf{r})|x,\ 0\rangle, \tag{24}$$

$$\lambda_{\pm}=\langle x,\ 0|\lambda_{\pm}(\mathbf{r})|x,\ 0\rangle, \tag{25}$$

$$W_{\pm}=-4\langle y,\ (011)|\hat{h}_{\pm}|z,\ 0\rangle, \tag{26}$$

$$\eta_1^{\pm}=4\langle y,\ (011)|\hat{h}_{\pm}|y,\ 0\rangle,\ \eta_2^{\pm}=4\langle y,\ (101)|\hat{h}_{\pm}|y,\ 0\rangle, \tag{27}$$

$$\xi_0=2\langle x,\ (100)|\hat{h}|x,\ 0\rangle,\ \xi_1=2\langle z,\ (100)|\hat{h}|z,\ 0\rangle. \tag{28}$$

The operator $\hat{\lambda}_{\pm}$ in (25) is defined by Eq. (10) in which $V(\mathbf{r})$ must be replaced by $\mathscr{V}(\mathbf{r})\mp\Delta(\mathbf{r})$ [see (14) and (15)].

The unitary transformation that diagonalizes $\hat{\mathscr{H}}_{\pm}=H_{\pm}(\mathbf{k}=0)$, is more conveniently carried out in two stages. We first transform to the basis $X_{\pm}^{(+)}\equiv(X^{(\pm)}\pm iY^{(\pm)})/\sqrt{2}, Z^{(\pm)}$:

$$\begin{pmatrix} X_{-}^{(\pm)} \\ Z^{(\pm)} \\ X_{+}^{(\pm)} \end{pmatrix}=\frac{1}{\sqrt{3}}\begin{pmatrix} e^{-\varphi} & e^{\varphi} & 1 \\ 1 & 1 & 1 \\ e^{\varphi} & e^{-\varphi} & 1 \end{pmatrix}\begin{pmatrix} \varphi_x^{\pm} \\ \varphi_y^{\pm} \\ \varphi_z^{\pm} \end{pmatrix}, \tag{29}$$

where $\varphi\equiv 2\pi i/3$. The functions $X^{(-)}, Y^{(-)}, Z^{(-)}$ are transformed in the D_{3d} group as polar-vector components defined in a coordinate frame with axes along the directions $(-1, -1.2), (1.-1.0)$ and (111). The functions $X^{(+)}, Y^{(+)}, Z^{(+)}$ transform in exactly the same way, apart from the inversion operation, with respect to which they are even. The transformation (29) diagonalizes the spin-independent part of the Hamiltonian.

In the second stage, account is taken of the SO interaction [the spin quantization axis is directed along (1,1,1) after the transformation (29)];

$$\begin{pmatrix} \hat{A}(\theta_{\pm}) & & \\ & \hat{A}\left(\theta_{\pm}-\frac{\pi}{2}\right) & \\ & & \hat{1} \end{pmatrix}\begin{Vmatrix} X_{-}^{(\pm)}\uparrow \\ Z^{(\pm)}\downarrow \\ Z^{(\pm)}\uparrow \\ X_{+}^{(\pm)}\downarrow \\ X_{+}^{(\pm)}\uparrow \\ X_{-}^{(\pm)}\downarrow \end{Vmatrix}=\begin{Vmatrix} \varphi_1^{\pm} \\ \varphi_2^{\pm} \\ \hat{K}\varphi_1^{\pm} \\ \hat{K}\varphi_2^{\pm} \\ X_{+}^{(\pm)}\uparrow \\ X_{-}^{(\pm)}\downarrow \end{Vmatrix}, \tag{30}$$

where $\hat{A}(\theta)$ is the two-dimensional-rotation matrix:

$$\hat{A}(\theta)=\begin{pmatrix} \cos\theta & \sin\theta \\ -\sin\theta & \cos\theta \end{pmatrix}. \tag{31}$$

The parameters $\theta_{\pm}$ are defined by the relations

$$\sin\theta_{\pm}=\alpha_{\pm}/(1+\alpha_{\pm}^2)^{1/2},\quad \cos\theta_{\pm}=1/(1+\alpha_{\pm}^2)^{1/2}, \tag{32}$$

$$\alpha_{\pm}=(3W_{\pm}+\lambda_{\pm}+[9W_{\pm}^2+6W_{\pm}\lambda_{\pm}+9\lambda_{\pm}^2]^{1/2})/2\sqrt{2\lambda_{\pm}}. \tag{33}$$

The functions in the right-hand column of (30) are the eigenfunctions of the Hamiltonian $\mathscr{H}_{\pm}$ (11). To each eigenvalue (12) corresponds a Kramers-conjugate pair ($\hat{K}$ is the Kramers operator).

The **k**-dependent terms in (22) lead to increments quadratic in **k** to the eigenvalues (13):

$$\varepsilon_i^{\mp}(\mathbf{k})=\varepsilon_i^{\mp}\pm\frac{\hbar^2k_{\parallel}^2}{2M_{\parallel}^{\mp}(i)}\pm\frac{\hbar^2k_{\perp}^2}{2M_{\perp}^{\mp}(i)}, \tag{34}$$

where $k_{\parallel}=\mathbf{k}\cdot\mathbf{n}$ and $k_{\perp}=k_x+ik_y$ are the components of **k** in the XYZ coordinate frame. Either the upper or the lower sign is taken in (34).

The masses $M(i)$ are determined by the overlap integrals in the second CS:

$$\begin{aligned}(M_{\parallel}^{\pm}(0))^{-1}&=\left(\frac{a}{\hbar}\right)^2\left(\frac{2W_{\pm}}{3}+2\varkappa_{\pm}\right),\\ (M_{\perp}^{\pm}(0))^{-1}&=\left(\frac{a}{\hbar}\right)^2\left(\frac{2W_{\pm}}{3}-\varkappa_{\pm}\right),\end{aligned} \tag{35}$$

$$\begin{aligned}(M_{\parallel}^{\pm}(1,2))^{-1}&=\left(\frac{a}{\hbar}\right)^2\left[W_{\pm}\left(\pm\frac{1}{3}-\cos 2\theta_{\pm}\right)+2\varkappa_{\pm}\right],\\ (M_{\perp}^{\pm}(1,2))^{-1}&=\left(\frac{a}{\hbar}\right)^2\left[W_{\pm}\left(\pm\frac{1}{3}-\cos 2\theta_{\pm}\right)-\varkappa_{\pm}\right],\end{aligned} \tag{36}$$

where $\kappa_{\pm}=(\eta_2^{\pm}+2\eta_1^{\pm})/3$; the upper and lower signs of $1/3$ correspond to the bands $\epsilon_1^{\pm}$ and $\epsilon_2^{\pm}$, respectively.

The obvious property $\hat{A}(\alpha)\hat{A}(\beta)=\hat{A}(\alpha+\beta)$ of the rotation matrices (31) facilitates the transformation of the off-diagonal block (20) to the basis (30). As a result we get

$$\hat{\xi}'=\begin{Vmatrix} P_{\parallel}\hat{A}(\delta) & P_{\perp}\hat{A}\left(\delta-\frac{\pi}{2}\right) & P_{\perp}^{*}\hat{A}(\theta_{-}) \\ P_{\perp}^{*}\hat{A}\left(\delta-\frac{\pi}{2}\right) & P_{\parallel}\hat{A}(\delta) & P_{\perp}\hat{A}\left(\theta_{-}-\frac{\pi}{2}\right) \\ P_{\perp}\hat{A}(-\theta_{+}) & P_{\perp}^{*}\hat{A}\left(-\theta_{+}-\frac{\pi}{2}\right) & P_{\parallel}\hat{1} \end{Vmatrix}. \tag{37}$$

Here $\delta=\theta_{-}-\theta_{+}$ and $P_{\parallel}=p_{\parallel}k_{\parallel}$, $P_{\perp}=p_{\perp}k_{\perp}$. The matrix elements $p_{\parallel,\perp}$ are expressed in terms of the bare spectrum (3)

$$p_{\parallel}=(\xi_0+2\xi_1)/\sqrt{3},\quad p_{\perp}=(\xi_0-\xi_1)/\sqrt{6}. \tag{38}$$

The matrix (37) is in essence the **k·p** Hamiltonian in the representation of the L-point eigenfunctions. Comparing it with the analogous expressions in Refs. 13 and 14, we can relate the phenomenological constants of the **k·p** theory with our parameters.

In all the considered compounds, the forbidden band is made up of the levels ϵ_2^{-} and $\epsilon_1^{\pm}$ (Fig. 3):

$$\varepsilon_g=\varepsilon_2^{-}-\varepsilon_1^{+}. \tag{39}$$

By perturbation theory we obtain from (37) the effective masses $m_{\parallel,\perp c}$ and $m_{\parallel,\perp v}$ on the bottom of the conduction band and on the top of the valence band, respectively:

$$\frac{1}{m_{\perp c}}=2\left(\frac{a\mathscr{P}_{\perp}}{\hbar}\right)^2\left[\frac{1}{\varepsilon_g}\cos^2\delta+\left(\frac{\sin^2\delta}{\varepsilon_2^{-}-\varepsilon_2^{+}}+\frac{1}{\varepsilon_2^{-}-\varepsilon_0^{+}}\right)\right]+\frac{1}{M_{\perp}^{-}(2)}, \tag{40}$$

$$\frac{1}{m_{\perp v}}=2\left(\frac{a\mathscr{P}_{\perp}}{\hbar}\right)^2\left[\frac{1}{\varepsilon_g}\cos^2\delta+\left(\frac{\sin^2\delta}{\varepsilon_1^{-}-\varepsilon_1^{+}}+\frac{1}{\varepsilon_0^{-}-\varepsilon_1^{+}}\right)\right]+\frac{1}{M_{\perp}^{+}(1)} \tag{41}$$

$$\frac{1}{m_{\parallel c}}=2\left(\frac{a\mathscr{P}_{\parallel}}{\hbar}\right)^2\left[\frac{1}{\varepsilon_g}\sin^2\delta+\left(\frac{\cos^2\delta}{\varepsilon_2^{-}-\varepsilon_2^{+}}\right)\right]+\frac{1}{M_{\parallel}^{-}(2)}, \tag{42}$$

$$\frac{1}{m_{\|v}}=2\left(\frac{a\mathscr{P}_\|}{\hbar}\right)^2\left[\frac{1}{\varepsilon_g}\sin^2\delta+\left(\frac{\cos^2\delta}{\varepsilon_1^--\varepsilon_1^+}\right)\right]+\frac{1}{M_\|^+(1)}. \quad (43)$$

In the six-band **k·p** theory,[14] Eqs. (40)–(43) contain in place of the correction masses $M_{\|,\perp}^{\pm}(i)$ the free-electron mass m_0. Yet, as seen from (35) and (36), these masses can be even negative and in no way connected with m_0. This means that allowance for the contribution $1/m_0$ is within the framework of the finite-band **k·p** method an exaggeration of the accuracy, since the unaccounted-for remote bands make a contribution of the same order. The published statements[17] that the term $1/m$ is significant are therefore invalid.

If all L-levels except ϵ_2^- and ϵ_1^+ are taken into account by perturbation theory, the dispersion near ϵ_g is described by the equation[1,13]

$$\left(-\varepsilon+\frac{\varepsilon_g}{2}+\frac{\hbar^2k_\perp^2}{2m_{c\perp}^*}+\frac{\hbar^2k_\|^2}{2m_{c\|}^*}\right)\left(-\varepsilon-\frac{\varepsilon_g}{2}-\frac{\hbar^2k_\perp^2}{2m_{v\perp}^*}-\frac{\hbar^2k_\|^2}{2m_{v\|}^*}\right)$$
$$=a^2(\mathscr{P}_\perp^2k_\perp^2+\mathscr{P}_\|^2k_\|^2). \quad (44)$$

The correction masses $m_{c,v}^*$ are determined by Eqs. (40)–(43) from which the contribution of the closest terms (the first term in the square brackets) must be omitted. The matrix elements $\mathscr{P}_{\|,\perp}$ differ from $p_{\|,\perp}$ (38) in accordance with the SO mixing:

$$\mathscr{P}_\|=p_\|\sin\delta, \quad \mathscr{P}_\perp=p_\perp\cos\delta. \quad (45)$$

In our approximation, $\mathscr{P}_\|$ and $\mathscr{P}_\perp$ depend only on the difference $\theta_- - \theta_+\equiv\delta$, but not on $\theta_\pm$ themselves. In the **k·p** scheme this is in general not the case,[14] owing to the larger number of unknown momentum matrix elements.

4. PHYSICAL MEANING AND NUMERICAL VALUES OF THE PARAMETERS

The ionization energy I_{IV} of the metal is lower than that of the chalcogenide I_{VI}. Therefore $\Delta(\mathbf{r})>0$ on the IV sites and $\Delta(\mathbf{r})<0$ on the VI sites. Consequently, $\Delta>0$ (24) (the origin is on the metal) and the states Γ^- lie lower than Γ^+ (if the origin is transferred to the VI site, the sign of Δ and the parities of the functions are reversed). As a result the odd states made up of the metal (IV) orbitals [see (21)] pertain to the conduction band while the even ones (from the chalcogen (VI) orbitals) to the valence bands.

Since

$$\hat{h}_-(\mathbf{r})=H(\mathbf{r}), \quad \hat{h}_+(\mathbf{r})=H(\mathbf{r}+\boldsymbol{\tau}),$$

the quantities W_+ and W_- in (26) are determined respectively by the overlap integrals of the functions from the VI or IV sublattices. For the same reason λ_+ and λ_- (25) should be close to the SO parameters of the chalcogen and metal atoms.

Since $\lambda_\pm>0$, the relative placement of the L levels (12) depends only on the sign of $W_\pm$. Therefore the inversion of the terms $\epsilon_2^-(L_2^{6'})$ and $\epsilon_0^-(L_3^{45'})$ with increasing λ_-, proposed in Ref. 18, is impossible.[6)]

Inserting in (12) the term positions calculated by various numerical methods[6,20,21] (a review of the band calculations is contained in Ref. 22) we can determine the parameters Δ, $W_\pm$, and $\lambda_\pm$ (see Table I).

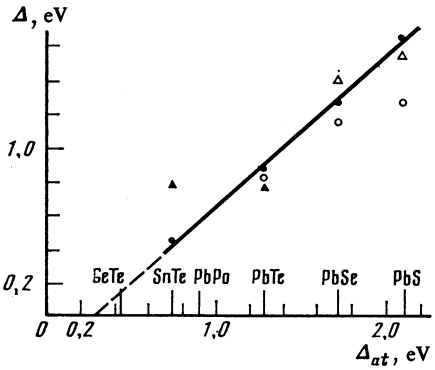

FIG. 4. Dependence of ionicity parameter on the half-difference of the energies of the atomic p triplets (without allowance for their spin-orbit and electrostatic splittings); ●—values assumed by us, ○—values of Δ calculated from the data of Ref. 6, ▲—from the data of Ref. 20, △—Ref. 21.

We note that the restriction

$$(\varepsilon_1-\varepsilon_2)/(\varepsilon_0-\varepsilon_1)>\sqrt{3}+1, \quad (46)$$

which follows from (12),[7)] makes certain data of Ref. 22 invalid, thus indicating that the corresponding calculations were not accurate enough. Within the limits of the scatter due to the difference between the data of Refs. 6, 20, and 21, the constants $\lambda_\pm$ turned out to be equal to the atomic SO parameters. Table I lists therefore the values of $\lambda_\pm$ calculated for neutral atoms by Herman and Skillman.[23]

The atomic analog of ionicity is half the difference of the p-term energies I_{IV}^* and I_{VI}^* without allowance for the spin-orbit and electrostatic splittings. They can be determined from the relation

$$I_{IV,VI}^*=\sum E_j^{IV,VI}\Big/\sum g_j^{IV,VI},$$

where $E_j^{IV,VI}$ are the energies of the optical terms for the electron configurations p_2 and p_4; $g_j^{IV,VI}$ are their degeneracy multiplicities. The ionicity calculated from (12) is found to be somewhat less than $\Delta_{a,t}=(I_{VI}^*-I_{IV}^*)/2$ (Fig. 4). This is due to the redistribution of the electron density among the atoms in the crystal.[24]

The intercenter integrals $W_\pm$, naturally, have no atomic analog. If the crystal potential in (26) is represented as a sum over the unit cells and the three-center integrals are neglected, as is customary, Eq. (26) will contain orbitals and potentials centered only on the VI and IV sublattices. One can therefore expect the change of W_- in the sequence Pb(S, Se, Te) or of W_+ for (Ge, Sn, Pb)Te to be due to the change of the lattice period. This is illustrated by Fig. 5, where the $W_\pm$ from Table I are plotted as functions of $a_0=2a$ (a_0 is the period of a lattice of the NaCl type).

Having determined from Fig. 5 the slopes of the straight lines $\partial W_\pm/\partial a$, it is easy to calculate the baric coefficients $\partial\epsilon_g/\partial p$. The theoretical values in Table I agree well with experiment.[17] The calculation of the strain potentials is perfectly analogous.

The parameters ξ_0 and ξ_1 were determined from the experimental values of the effective masses with the aid of relations (38) and (40)–(43). The contribution of the correction masses $M(i)$ turns out to be small (for PbTe, $\varkappa_+\approx0.1$ eV

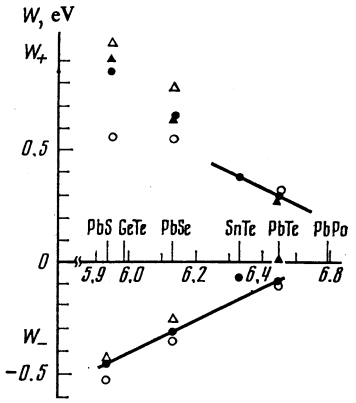

FIG. 5. Dependence of the hybridization parameters on the lattice period: ●—values assumed by us, ○—values of $W_{\pm}$ calculated from the data of Ref. 6, ▲—from the data of Ref. 7, △—Ref. 21.

(Ref. 5) and $M_{\perp} \sim 4m_0$), and that $\varkappa_{\pm}$ cannot be reliably determined. It is interesting that quantities ξ_0, ξ_1, and $(W_+ + W_-)/2$ pertaining to the parent phase are practically the same for all IV–VI compounds.

From the set of parameters obtained for binary compounds we can calculate the band structures of multicomponent solid solutions. In the virtual-crystal approximation[25] the matrix elements (24)–(28) for an alloy $A_x B_{1-x} C$ are expressed in terms of the values for the corresponding binary solutions:

$$V = V_{AC}x + V_{BC}(1-x). \tag{47}$$

Figures 6 and 7 show the calculated $g(x)$ and effective-mass anisotropy coefficient $K = m_{\parallel}/m_{\perp}$.

Attention is called to the strongly nonlinear relations in the alloys $A^{IV} B^{VI}_{1-x} C^{VI}_x$; these relations agree well with the experimental data for $PbSe_{1-x}Te_x$.[18,19] It must be emphasized that this nonlinearity occurs for a linear variation of the parameters (47) and is not accompanied by inversion of the terms L_2' and L_3'. The linearity of the $\epsilon_g(x)$ dependences in the alloys $Pb_{1-x}Sn_xTe(Se)$ is also confirmed by experiment (Refs. 26, 27).[8)]

With increasing x in the $Pb_{1-x}Sn_xTe$ alloys, the terms $L^{6'}$ and L^6, which form the forbidden band, are inverted (Fig. 6), and this leads to a nonmonotonic change of $m_{\parallel,\perp}$. In a definite composition region, the interaction with the remote

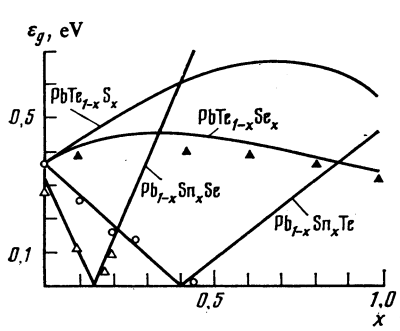

FIG. 6. Dependence of the forbidden-band gap on the composition in ternary solid solution. Experimental data of: ▲—Ref. 18, ○—Ref. 26, △—Ref. 27.

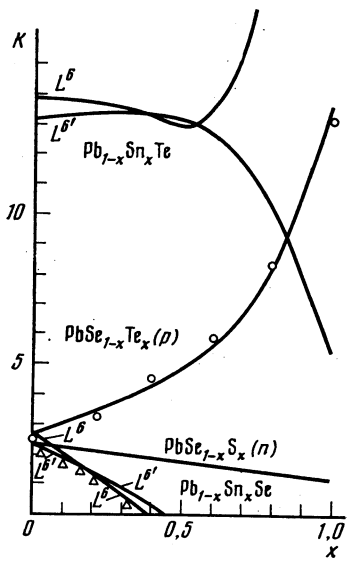

FIG. 7. Variation of the anisotropy coefficient $K = m_{\parallel}/m_{\perp}$ for electrons (n) and holes (p) in solid solutions. Experimental data: ○—Ref. 19, △(n type)—Refs. 28 and 29.

terms $L^{45'}$ and $L^{6'}$ cancel out the direct interaction of L^6 and $L^{6'}$, after which $m_{\parallel}$ and subsequently $m_{\perp}$ become infinite. As $m_{\parallel} \to \infty$ the anisotropy coefficient $K \to \infty$ (Fig. 7). The spectrum is determined by the terms ∞ $\mathbf{k}^4$ and Eq. (44) is incorrect. The first to become infinite in $Pb_{1-x}Sn_xSe$ is m, and consequently $K \to 0$, as is confirmed by experiment (a structural transition into the orthorhombic phase takes place in $Pb_{1-x}Sn_xSe$ at $x > 0.40$).

From the regularities established we can determine the band structure of PbPo, a compound whose energy spectrum was not investigated in experiment. It is known that PbPo has an NaCl lattice with a period $a_0 = 6.59$ Å.[30] The value of I^*_{Po} (Fig. 4) can be determined by linear interpolation of the plot of $I^*_{VI}(I_{VI})$ for the chalconide series (S, Se, Te, Po). Owing to the large lattice period, the hydridization is extremely small (Fig. 5), and the SO interaction, to the contrary, is large: $\lambda_+ = 0.7$ eV. Therefore the order of the terms at the L point is unusual (Fig. 8). The band extrema lie on the intersection lines of the corrugated Fermi surfaces (Fig. 1). The electronic minima (their number is 24) are strongly displaced from the L points, and the hole maxima are located

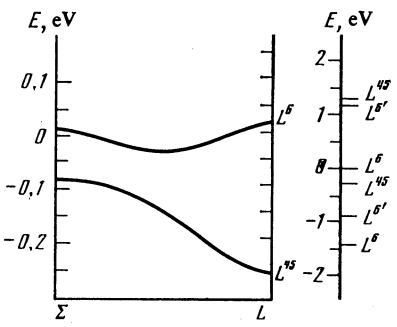

FIG. 8. Energy spectrum of PbPo. The dispersion is shown only for the lower conduction band and the upper valence band. On the right is shown the arrangement of the levels at the L points.

near the points of intersection of the indicated lines with the Σ (110) axes (Fig. 8). A similar picture of the band structure of PbPo was obtained by the augmented-plane-wave method,[31] but there the electron extremum was related to the L point. The Σ extremum of the valence band, which is the principal one in PbPo, appears as a secondary in PbTe.[17] Calculation shows that its position in SnTe is practically equal to that of the L extremum of the valence band.

5. CONCLUSION

The first (symmetry) stage of the approach expounded here is based on using a triply degenerate p state as the bare level at the L point. This raising of the point symmetry is similar to the translational-symmetry raising on which the Abrikosov-Fal'kovskiĭ method[9] is based. This decreases the number of independent momentum matrix elements in the **k·p** system to four, owing the equality of the radii (r_{IV}, r_{VI}) of the wave functions in the parent phase. The fact that these radii are in fact different ($r_{IV}/r_{VI} \approx (I_{IV}/I_{VI})^{1/2} \approx 1 + \Delta/I \approx 1.1$) reduces, in the calculation of the IV–VI spectrum from the parent phase, to allowance for the contribution from the remote bands.

The second (model) stage of our approach is connected with the use of the tight-binding approximation. This has greatly decreased the number of the parameters of the theory and made it possible to determine their connection with the atomic characteristics. It was found that the available experimental data are well described by the theory if account is taken of overlap integrals with two nearest coordination spheres. The integral of the first sphere is related to that of the second like $W/\xi_0 \sim 0.1$ (see Table I). This suggests that the overlap integrals of the third coordination sphere introduce corrections not larger than 1% into the IV–VI spectrum. If only two coordination spheres are taken into account the difference between the atomic radii of the IV and VI elements does not enter at all in the determination of the parameters of the theory, and the number of independent momentum matrix elements in the **k·p** theory is reduced to two.

[1)]For example, calculations by the pseudopotential method for PbTe (Ref. 6), Bi (Ref. 7), and Te (Ref. 8).

[2)]In analogy with Bi and Te, noncubic lattices of IV–VI compounds are obtained by distortions of a structure of the NaCl type.[2]

[3)]A similar approach, which connects the spectra of diamond-like semiconductors and of compounds with zincblende structure, is known as the Herman perturbation method.[11] In this case, however, Δ (r) has the translational symmetry of the "parent phase" and differs from it only in that it is not invariant to inversion.

[4)]The group C_{3v} has two one-dimensional (A_1, A_2) and one two-dimensional (E) irreducible representations.

[5)]In contrast to bismuth, where the smallest of these parameters is probably Δ_{ph}.

[6)]This assumption was invoked by Akopyan *et al.*[19] to explain the nonlinear dependence of the anisotropy coefficient in the $PbTe_{1-x}Se_x$ alloy. It will be shown below that this assumption is unnecessary.

[7)]Relations (12) and (46) are of symmetry origin. They are due to the genesis of the terms L_3^+, L_1^+ and L_3^-, L_2^- from two triplets of p-like Wannier orbitals. The accuracy of (12) and (46) is therefore determined by the smallness of the $W_\pm$ hybridization relative to the distance to other remote p-type bands ($\sim 10^{-2}$).

[8)]In post-inversion compounds $Pb_{1-x}Sn_xSe$ one can have deviations from nonlinearity because of the nonlinear change of the lattice period near the point of the phase transition into the orthorhombic phase.

[1]I. M. Tsidil'kovskii, Zonnaya struktura poluprovodnikov (Band Structure of Semiconductors), Nauka, p. 126 (1978).
[2]B. A. Volkov and O. A. Pankratov, Zh. Eksp. Teor. Fiz. **75**, 1362 (1978) [Sov. Phys. JETP **48**, 687 (1978)].
[3]B. A. Volkov and O. A. Pankratov, FIAN Preprints 127 and 130 (1980).
[4]B. A. Volkov, V. P. Kushnir and O. A. Pankratov, Fiz. Tverd. Tela (Leningrad) **24**, 415 (1982) [Sov. Phys. Solid State **24**, 235 (1982)].
[5]B. A. Volkov, O. A. Pankratov and A. V. Sazonov, Fiz. Tekh. Poluprovodn. **16**, 1734 (1982) [Sov. Phys. Semicond. **16**, 1112 (1982)].
[6]L. Kleinman and P. Lin, Phys. Rev. **142**, 478 (1966).
[7]S. Golin, Phys. Rev. **166**, 643 (1968).
[8]K. Maschke, Phys. Stat. Sol. (b) **47**, 511 (1971).
[9]A. A. Abrikosov and L. A. Fal'kovskiĭ, Zh. Eksp. Teor. Fiz. **43**, 1089 (1962) [Sov. Phys. JETP **16**, 769 (1963)].
[10]S. A. Gordyunin and L. I. Gor'kov, Pis'ma Zh. Eksp. Teor. Fiz. **20**, 668 (1974) [JETP Lett. **20**, 307 (1974)].
[11]F. Herman, Electronics No. 1, 103. (1955).
[12]A. A. Abrikosov, Zh. Eksp. Teor. Fiz. **65**, 2063 (1973) [Sov. Phys. JETP **38**, 1031 (1974)].
[13]J. O. Dimmock and G. V. Wright, Phys. Rev. **135**, A821 (1964).
[14]D. L. Mitchell and R. F. Wallis, Phys. Rev. **151**, 581 (1966).
[15]J. Zak, Phys. Rev. **B23**, 2824 (1981).
[16]J. C. Slater and G. F. Koster, Phys. Rev. **94**, 1498 (1954).
[17]Yu. I. Ravich, B. A. Efimova and I. A. Smirnov, Metody issledovania poluprovodnikov v primenenii k khal'kogenidam svintsa PbTe, PbSe i PbS. (Methods of Investigating Semiconductors as Applied to Lead Chalcogenides PbTe, PbSe, and PbS) Nauka, 306 (1968).
[18]A. Jedrzejczak, D. Guillot and G. Martinez, Phys. Rev. **B17**, 829 (1978).
[19]E. A. Akopyan, G. A. Galandarov, A. Sh. Mekhtiev, and F. E. Faradzhiev, Fiz. Tekh. Poluprovodn. **15**, 2012 (1981) [Sov. Phys. Semicond. **15**, 692 (1981)]. Fiz.Tverd. Tela (Leningrad) **24**, 971 (1982) [Sov. Phys. Solid State **24**, 552 (1982)].
[20]K. Bernick and L. Kleinman, Sol. St. Comm. **8**, 569 (1970).
[21]S. E. Kohn, R. Y. Yu., Y. Petroff, Y. R. Shen, Y. Tsang and M. L. Cohen, Phys. Rev. **B8**, 1477 (1973).
[22]V. V. Sobolev, Sobstvennye energeticheshie urovni soedinenii gruppy $A^{IV}B^{VI}$ (Energy eigenlevels of IV–VI Compounds), Kishinev: Shtinitsa, p. 11 (1981).
[23]F. Herman and S. Skillman, Atomic Structure Calculations. Prentice-Hall Inc., Englewood Cliffs, New Jersey, pp. 2–6 (1963).
[24]B. A. Volkov and V. P. Kushnir, Fiz. Tverd. Tela (Leningrad) **25**, 1803 (1983) [Sov. Phys. Solid State **25**, 1038 (1983)].
[25]H. Ehrenreich and L. Schwarz, Electronic Structure of Alloys (Russ. transl.), Nauka, 1979, p. 8.
[26]J. O. Dimmock, I. Melngailis and A. J. Strauss, Phys. Rev. Lett. **16**, 1193 (1966).
[27]J. Melngailis, T. C. Harman and W. C. Kernan, Phys. Rev. **B5**, 2250 (1972).
[28]I. V. Kucherenko, A. E. Svistov and A. P. Shotov, Fiz. Tekh. Poluprovodn. **15**, 2111 (1981) [Sov. Phys. Semicond. **15**, 1226 (1981)].
[29]K. V. Vyatkin, I. V. Kucherenko, V. I. Moiseenko and A. P. Shotov, Fiz. Tekh. Poluprovodn. **11**, 1831 (1977) [Sov. Phys. Semicond. **11**, 1074 (1977)].
[30]R. Dalven, J. Nonmetals **1**, 179 (1973).
[31]S. Rabii and R. H. Lasseter, Phys. Rev. Lett. **33**, 703 (1974).

Translated by J. G. Adashko